

Characterization of carboxylated cellulose nanofibrils and oligosaccharides from Kraft pulp fibers and their potential elicitor effect on the gene expression of *Capsicum annuum*

María Emilia Cano^{a,b}, Åsa Lindgren^c, Jennifer Rosendahl^c, Jenny Johansson^c, Alberto Garcia-Martin^d, Miguel Ladero Galan^d, José Kovensky^a, Gary Chinga-Carrasco^{e,*}

^a Laboratoire de Glycochimie, des Antimicrobiens et des Agroressources UR 7378, Université de Picardie Jules Verne, 80025 Amiens, France

^b CONICET-Universidad de Buenos Aires, Centro de Investigaciones en Hidratos de Carbono (CIHIDECAR), Departamento de Química Orgánica, Facultad de Ciencias Exactas y Naturales, Universidad de Buenos Aires, Ciudad Universitaria, Pabellón 2, C1428EGA Buenos Aires, Argentina

^c RISE Methodology, Textile and Medical Device, Biological Function Unit, Box 857, 50115 Borås, Sweden

^d FQPIMA Group. Chemical Engineering and Materials Department, Universidad Complutense de Madrid. 28040 Madrid, Spain

^e RISE PFI, Høgskoleringen 6b, Trondheim, Norway

ARTICLE INFO

Keywords:

Nanocellulose
TEMPO-oxidized nanofibrils
Plant substrate
Elicitor
Oligosaccharides
Characterization

ABSTRACT

Biomass-derived oligo- and polysaccharides may act as elicitors, *i.e.*, bioactive molecules that trigger plant immune responses. This is particularly important to increase the resistance of plants to abiotic and biotic stresses. In this study, cellulose nanofibrils (CNF) gels were obtained by TEMPO-mediated oxidation of unbleached and bleached kraft pulps. The molecular structures were characterized with ESI and MALDI MS. Analysis of the fine sequences was achieved by MS and MS/MS of the water-soluble oligosaccharides obtained by acid hydrolysis of the CNF gels. The analysis revealed the presence of two families: one corresponding to homogluconic acid sequences and the other composed by alternating glucose and glucuronic acid units. The CNF gels, alone or with the addition of the water-soluble oligosaccharides, were tested on Chili pepper (*Capsicum annuum*). Based on the characterization of the gene expression with Next Generation Sequencing (NGS) of the *C. annuum*'s total messenger RNA, the differences in growth of the *C. annuum* seeds correlated well with the downregulation of the pathways regulating photosynthesis. A downregulation of the response to abiotic factors was detected, suggesting that these gels would improve the resistance of the *C. annuum* plants to abiotic stress due to, *e.g.*, water deprivation and cold temperatures.

1. Introduction

Plants produce low molecular weight bioactive compounds that trigger a response reaction to biotic and abiotic stresses. Such compounds are called elicitors and can be released from the plant cell wall as small polysaccharide fragments [1–3]. These endogenous oligosaccharides can be applied as an environmentally-sound alternative to pesticides. In recent years, numerous oligosaccharides have been identified as elicitors in a wide variety of plants [4]. Glucuronans and oligoglucuronans, for instance, produced defense responses in apple fruits and grapevine [5,6]. Additionally, the elicitor activity in *Arabidopsis thaliana* of cellulose and hemicellulose-derived oligosaccharides has been studied in detail [7]. However, challenges regarding the obtention of

oligosaccharides from plants motivate the development of new technologies in this area.

Oligosaccharides can be obtained by depolymerization of polysaccharides from natural sources. Autohydrolysis, acid/basic hydrolysis and enzymatic depolymerization are the three common techniques to produce these kind of sugars [8]. For example, arabinooligosaccharides were produced from beet fibers by autohydrolysis [9]; oligogalacturonans with elicitory properties [2], were obtained and characterized from agro-food wastes by treatment of two sequential acid hydrolysis steps using HCl and TFA [10]; and xilooligosaccharides were produced using basic conditions in the extraction of xylan from hardwood [11]. On the other hand, the enzymatic process is mainly mediated by hydrolases and lyases with milder conditions than those mentioned above

* Corresponding author.

E-mail address: gary.chinga.carrasco@rise-pfi.no (G. Chinga-Carrasco).

<https://doi.org/10.1016/j.ijbiomac.2024.131229>

Received 1 August 2023; Received in revised form 7 March 2024; Accepted 27 March 2024

Available online 9 April 2024

0141-8130/© 2024 The Authors. Published by Elsevier B.V. This is an open access article under the CC BY license (<http://creativecommons.org/licenses/by/4.0/>).

(adequate pH and temperature) [8,12]. To be applicable, these methods must be reproducible, and the mixtures must be properly characterized to provide insights about the most active structures.

The cell wall of plants is composed of cellulose microfibrils as the structural component. In the case of wood, microfibrils can be released from the wood tracheids through a series of pulping and post-treatment processes, thus giving rise to large-scale production of cellulose nanofibrils (CNF). One of the most common processes to obtain CNF is from chemical pulps (e.g. kraft pulps), applying 2,2,6,6-tetramethylpiperidinyl-oxyl (TEMPO)-mediated oxidation with NaClO as co-oxidant, which is used to regenerate the TEMPO catalyst [13,14]. TEMPO CNF gels have a range of interesting properties such as tunable surface chemistry, homogeneous nanofibril morphology, high viscosity at low concentration, biocompatibility, antibacterial properties and can form films with high translucency and strength [15–17]. Hence, TEMPO CNF gels have been proposed for a series of high-end applications, including tissue engineering, wound dressings and biological tissue models [18–21]. CNF gels may also contain oligosaccharides and these may act as elicitors for plant cultivation, which is an area of limited research.

Previously, CNF has been proposed as substrate for plant cultivation [22] and complemented with salicylic acid as potential elicitor [23]. Salicylic acid has the potential to increase the resistance of plants to, e.g., abiotic and biotic (pathogens) stresses [24]. Effector-triggered plant immunity can contribute to protecting plants. However, it is difficult to assess the effect of elicitors as this would usually require extensive plant trials. One plausible way of assessing the effect of elicitors on plants is to characterize the genetic response of the plants as they are exposed to a given substrate or treatment. This can be done by characterizing the gene expression with Next Generation Sequencing (NGS) of the plant's total mRNA (RNA sequencing). The expression of genes is defined by the depth of coverage of the corresponding sequence aligned with a reference genome. Differences in gene expression between two or more conditions (treatments, growth conditions etc.) is determined by analysis of significant fold changes of read counts between conditions [25].

In July 2015 NASA announced the cultivation of chili pepper plants (*Capsicum annuum*) in the international space station (ISS). This would be the first fruit to be cultivated under microgravity. Chili pepper is particularly interesting due to the limited height of the plant, the short growing period and the high content of vitamin C, a powerful antioxidant [26]. In 2022, NASA announced the successful cultivation of this plant in microgravity in the ISS [27]. This milestone expands the range of plants with potential to be cultivated in space for the foreseen space exploration, i.e., establishing facilities on the Moon as a step for the long-term travelling to Mars. Such initiatives emphasize the relevance of *C. annuum* as a model plant for assessing substrates for plant cultivation *in vitro* and how these substrates can be expected to influence plant growth.

According to Larskaya and Gorshkova [3], two main challenges exist regarding the development of oligosaccharides as elicitors: 1) relevant structural characterization of individual oligosaccharides, and 2) develop relevant test systems. Additionally, we hypothesized that the TEMPO CNF gels contained oligosaccharides potentially caused by hydrolysis and β -elimination during the TEMPO mediated oxidation at pH 10 [15,28,29], and due to the mechanical homogenization process. TEMPO oligosaccharides (containing carboxylic acid and aldehyde groups) could cause a distinct effect on the physiological behavior of plants, by acting as elicitors. Hence, the purpose of this study was to confirm the occurrence of oligosaccharides in CNF gels and to address the mentioned challenges by: 1) developing a new method to obtain oligosaccharides in relatively large quantities based on additional acid hydrolysis of TEMPO CNF gels, 2) perform a comprehensive structural characterization of the oligosaccharides by mass spectrometry and 3) demonstrate the effect of the oligosaccharides by state-of-the-art gene sequencing analysis.

Table 1

CNF gels obtained from pulp fibers.

| Code | Kraft pulp | NaClO ($\mu\text{mol/g}$) |
|----------|------------|-----------------------------|
| uCNF_3.8 | Unbleached | 3800 |
| bCNF_3.8 | Bleached | 3800 |
| uCNF_6.0 | Unbleached | 6000 |
| bCNF_6.0 | Bleached | 6000 |

2. Materials and methods

2.1. Materials

Unbleached and bleached kraft pulp fibers (*Pinus radiata*, CMPC Chile) were used as raw material for obtaining CNF and oligosaccharides. TEMPO (Aldrich, 98 % purity), NaBr (Sigma-Aldrich, >99 % purity), NaClO (hypochlorite, Roth, 12 % technical), HCl (0.5 M, Roth) and NaOH (0.5 M, Roth) were applied for CNF production.

99 % Ammonium formate, 37 % HCl and 96 % ethanol were bought from Acros Organics. D-(+)-glucose, D-(+)-xylose, D-(+)-mannose, D-(-)-arabinose, L-(+)-rhamnose and H₂SO₄ 98 % were purchased to Sigma-Aldrich. Water used for HPAEC experiments was of very low conductivity (MilliQ grade, 18 M Ω , Millipore, Bedford, MA). For MS, matrices and calibrating chemicals were purchased from Sigma-Aldrich.

2.2. Carboxylated CNF

Bleached (100 g) and unbleached pulp fibers (100 g) were pre-treated with TEMPO-mediated oxidation and using 3.8 and 6.0 mmol NaClO [30]. The codes of the four produced series are given in Table 1. TEMPO (1.25 g) and NaBr (12.5 g) were dissolved in water and added to the kraft pulp, before dropwise addition of NaClO (3.8 or 6.0 mmol/g fibers). The pH was maintained at 10.5 by addition (dropwise) of NaOH (0.5 M, Roth). The reaction time was approx. 2 h at room temperature (~20 °C). The pH was then adjusted to 7 by adding 0.5 M HCl, before dewatering of mother liquors through a filter (125 μm). Washing of the pre-treated pulp fibers was performed with Milli-Q water (resistance: 18.2 M Ω /cm) until the conductivity was <5 $\mu\text{S/cm}$. The washed fibers were passed 3 times through a homogenizer (Rannie 15 type 12.56 \times 9), using 1000 bar pressure. The concentration of the obtained CNF material was approx. 1 wt%.

Conductometric titration was applied to quantify the content of carboxylic acids, according to Saito and Isogai [13].

The carbohydrate composition of samples uCNF_3.8 and bCNF_3.8 was assessed following the protocol NREL/TP-510-42618 [31]. The samples (concentration of 0.4 wt%) were frozen at -80 °C and lyophilized for 24 h. The freeze-dried samples (uCNF_3.8 and bCNF_3.8) were milled with a blade homogenizer and sieved to obtain a particle size distribution between 0.18 and 0.88 mm, as described the NREL/TP-510-42620 [32]. Monomeric carbohydrates released by the total acid hydrolysis of the samples were quantified by anion exclusion HPLC. For this analysis 10 μL of sample (hydrolysis liquid, 4 % aqueous solution of H₂SO₄) was injected in a BP 800-H column (PS-DVB, 9 μm , 300 \times 7.8 mm) at flow rate of 0.5 mL/min of H₂SO₄ 5 mM in degassed MilliQ grade water (pH 2). The temperature of the column was set at 60 °C and the detection of analytes was carried out with a Refractive Index Detector (RID) at 40 °C. The lignin content was quantified by determining the Kappa number according to TAPPI/ANSI T 236 and then transformed to weight percentage multiplying by factor of 0.13 [33].

The CNF samples were diluted to 0.6 wt% for assessment of storage (G') and loss (G'') moduli. The rheological assessment was performed with a dynamic mechanical analyzer MCR 702e (Anton Paar GmbH, Graz, Austria). The strain sweep was performed to determine the linear viscoelastic region.

The CNF samples were diluted to 0.4 wt% and films (20 g/m²) were

made in petri dishes. The films were allowed to dry at room temperature (~20 °C). The dried films were scanned with a UV-visible spectrophotometer (Cary 300 Conc, Varian) to quantify the light transmittance between wavelengths of 200 and 800 nm.

2.3. Mass spectrometry

2.3.1. Electrospray ionization (ESI)

MS-detection was performed following the protocol used before [10]. SYNAPT G2-Si instrument hyphenated with the ACQUITY UPLC H-Class system was used (Waters, Manchester, UK). The ESI source was operated in the negative ionization mode using a capillary voltage of -2.5 kV and the following conditions: cone voltage, 120 V; source offset, 20 V; source temperature, 120 °C; desolvation gas temperature, 450 °C; desolvation gas flow, 800 L/h, and cone gas flow, 50 L/h. Nitrogen (> 99.5 %) was employed as the desolvation gas. Mass calibration was carried out using a sodium formate solution (10 mM NaOH in isopropanol/water/formic acid 49.9:49.9:0.2, v/v/v) and a lock mass correction was applied for accurate mass measurements using the $[M-H]^-$ ion (m/z 554.2615) obtained from a Leu-enkephalin solution (1 ng/ μ L in H₂O/CH₃CN/formic acid 50:49.9:0.1, v/v/v). The scan range was m/z 50–2500 at 0.25 s/scan. The TOF was operated in the sensitivity mode, providing an average resolving power of 20,000 (FWHM). All spectra were recorded in the continuum mode. Data acquisition was performed with MassLynx software (V4.1, Waters). For collision-induced dissociation (CID) experiments, argon was used as collision gas at an indicated analyzer pressure of 5.10^{-5} Torr and the collision energy was optimised for each parent ion (50–110 V).

2.3.2. Matrix assisted laser desorption ionization - time of flight (MALDI-TOF)

MALDI-TOF experiments were performed using a SYNAPT G2-Si hybrid quadrupole time-of-flight instrument (Q-TOF) equipped with an intermediate pressure (IP) MALDI ionization source (Waters, Manchester, UK). The source was operated with a 2.5 KHz solid state UV laser system ($\lambda = 355$ nm). HRMS data were recorded in the negative ion mode. Mass calibration from 50 to 4000 Da was carried out using 2-[(2E)-3-(4-*tert*-butylphenyl)-2-methylprop-2-enylidene] malononitrile (DCTB) matrix mixed with CsI₃ in a 1:2 M ratio in THF. The scan range was m/z 50–3000 at 1 s/scan. The TOF was operated in the sensitivity mode, providing an average resolving power of 20,000 (FWHM). The source parameters were as follow: sample plate, 30 V; extraction, 30 V; hexapole, 20 V and aperture, 5 V. The HRMS spectra were recorded in the continuum mode. Data acquisition was performed with MassLynx software (V4.1, Waters). MS/MS experiments were performed as described above.

The ionic liquid matrix (ILM) of HABA/TMG₂ used in this study was prepared as previously reported [34,35]. HABA (30 mg) was mixed with TMG (31.2 μ L) in methanol (300 μ L), and the resulting solution was sonicated for 15 min at 40 °C and dried under vacuum overnight. ILM was then prepared at a concentration of 70–90 mg/mL in methanol for use as a matrix, without further purification.

For the preparation of the samples 1–2 mg of the oligosaccharide fraction were dissolved in 500 μ L of water and Dowex 50 \times 8–400 ion exchange resin was added. Equal volumes of this solution and ionic liquid matrix were mixed. An amount of 1.3 μ L of the mixture was deposited on a mirror polished stainless steel MALDI target (Waters 405,010,856, 8 cm \times 12 cm, 96 well) and was air-dried at room temperature and atmospheric pressure for 2 h.

2.4. High performance anion exchange chromatography (HPAEC) analysis

HPAEC analysis was performed on a Waters autopurification system (Waters, France) equipped with a 1525 binary pump coupled to a SEDEX LT-ELSD LC detector (Sedere, France) set at 60 °C and a gain of 7. The

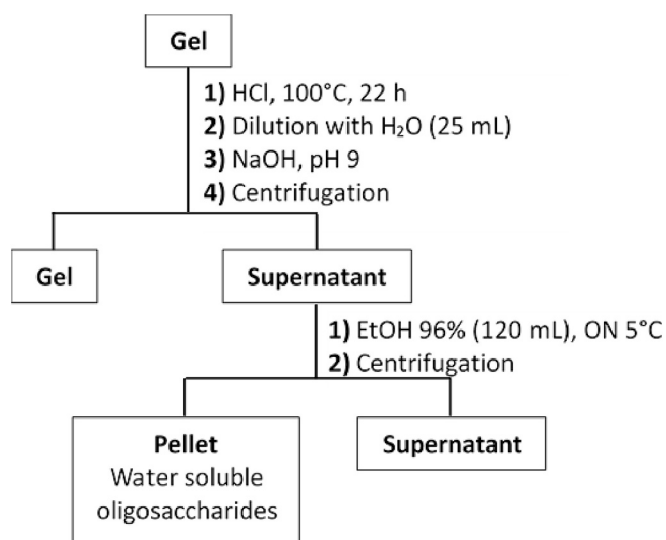


Fig. 1. Scheme of the hydrolysis and separation of water-soluble oligosaccharides.

run was performed at room temperature, the compounds were loaded on a TSKgel DEAE 5PW column (10 μ m particle size, 75 mm \times 7.5 mm) and the sample injection volume was 20 μ L (aqueous solution at 10 mg/mL). Ammonium formate (1 mM, A) and ammonium formate (1 M, B) were used as eluents. Gradient: 0–20 min (100:0 to 85:15 v/v), 20–60 min (85:15 to 62:38 v/v), 60.01–70 min (0:100 v/v) at a flow rate of 1 mL/min. Oligogalacturonic acids of different degree of polymerization were used as standards [10].

2.5. Gel hydrolysis

bCNF_6.0 (25 mL, 0.6%wt) gel was treated with HCl (37 %, 1.23 mL) at 100 °C for 22 h. After cooling to room temperature, water (50 mL) was added and the pH was adjusted to 9 with 4 M NaOH. Then, the mixture was centrifuged for 20 min at 9500 rpm to separate the gel that did not react. 96 % EtOH (160 mL) was added to the supernatant, and after 24 h at 5 °C, the precipitate was recovered as pellet by centrifugation and dried under vacuum at 40 °C (29.2 mg, 20 % yield) (Fig. 1).

The fraction of water-soluble oligosaccharides was analyzed by HPAEC and MS. A new sample was prepared by mixing 85 wt% uCNF_3.8 with 15 wt% of the water-soluble oligosaccharides from sample bCNF_6.0. This sample was homogenized with an Ultraturrax, 30 s at 24000 RPM (sample code uCNFO15), and was used to test the effect of oligosaccharides on the gene expression of chili plants.

2.6. Chili trials and gene expression

2.6.1. Cultivation and harvest

A schematic representation of the Chili plant trial and corresponding gene expression analysis is provided in Fig. 2. *C. annum* seeds were cultivated in 24-well plates, in three different CNF gels (uCNF_3.8, bCNF_3.8 and uCNFO15, concentrations = 0.6 wt%) covering approximately 2/3 of the seed. Commercial soil (Premium flower soil, Norway) was used as control. The seeds were cultivated during 14 days at room temperature and the circadian cycle: 16 h light and 8 h dark controlled by timer, where the dark period coincided with the dark hours of the day. Tap water was used for watering and to keep the CNF gels and soil constantly moist. The lids were removed when the first cotyledons were visible. Roots, stems and leaves were harvested together and immediately frozen in liquid nitrogen and stored at -80 °C until RNA extraction.

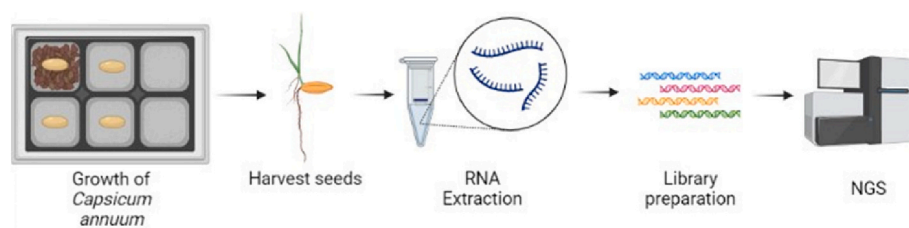


Fig. 2. Schematic representation of the gene sequencing analysis. Picture created in [biorender.com](https://www.biorender.com).

2.6.2. RNA extraction

The frozen *C. annuum* samples were homogenized with 5 mm steel beads in a TissueLyzer LT (Qiagen) for 5 min at 30 Hz. RNA was extracted using the Plant/Fungi Total RNA Purification kit (Norgen) with an on-column DNA removal step with the RNase-free DNase I kit (Norgen) according to the manufacturer's instructions. The samples were eluted in 25 μ L Elution A solution; RNA quality and concentration was determined using Nanodrop (ThermoFisher) and Qubit dsDNA HS assay (Agilent). The samples were stored at -80 °C until library preparation.

2.6.3. Library preparation for NGS

The extracted RNA samples were diluted in H_2O to 15 ng/ μ L and 10 μ L per sample were used for library preparation. Prior to library preparation poly(A) mRNA was generated, using the Poly(A) Selection Kit (Lexogen) according to manufacturer's instructions. Briefly, the total RNA was denatured at 60 °C and hybridized to magnetic beads selective for RNA with a poly(A) tail.

Single index (i7 indices only) library preparation was then performed using the Corall total RNA-seq Library prep kit (Lexogen) according to the manufacturer's instructions. The libraries were generated by reverse transcription into cDNA and amplification and indexing were made with PCR. The single indexing PCR was performed at 19 cycles as determined using the PCR Add-on Kit for Illumina (Lexogen) and libraries indexed using the Lexogen i7 6nt index set. The libraries were eluted in 20 μ L elution buffer and stored at -20 °C.

Size distribution of the libraries was analyzed using Bioanalyzer 2100 HS DNA kit (Agilent) according to manufacturer's instructions. An average size of the libraries of approximately 300 bp were expected and libraries with a side product visible at approximately 155 bp comprising >3 % of the total library were repurified with magnetic beads according to the manufacturer's instructions (Lexogen). Libraries were diluted 1:10000 and quantified with qPCR on a CFX96 (BioRad) using the NGS Library Quantification kit (TATAA) according to the manufacturer's instructions.

2.6.4. Sequencing and analysis

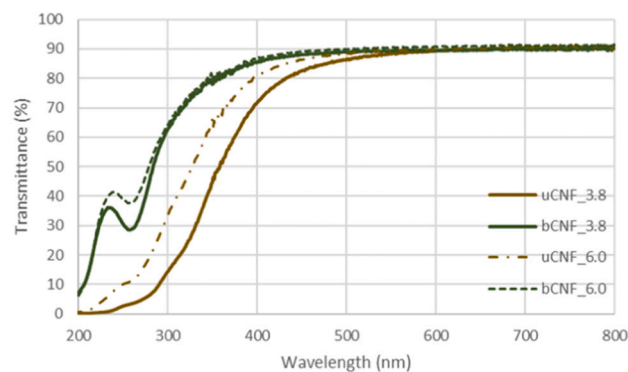
Libraries were diluted to 650pM, pooled and sequenced on a NextSeq2000 sequencer (Illumina). A 5 % PhiX spike-in (Illumina) was used as control.

The data were analyzed in BaseSpace (Illumina) using the DRAGEN RNA and DRAGEN Differential expression pipelines. The reads were aligned to *C. annuum* UCD-10 \times -F1 reference genome and differential gene expression was analyzed in comparison to the control samples (soil-grown).

Differential gene expression with an adjusted p -value of <0.05 was discarded and only genes with a raw count of >5 reads for at least two out of three replicates were considered valid. Pathway analysis was performed using STRING (string-db.org) using the multiple proteins setting and *C. annuum* as organism (Supplementary Fig. S1).



A



B

Fig. 3. Light transmittance of CNF films. (A) Self-standing films of samples uCNF_3.8, bCNF_3.8, uCNF_6.0 and bCNF_6.0. (B) UV-vis transmittance analysis.

3. Results and discussion

3.1. Characterization of CNF gels and films

Previously, we have extensively characterized the CNF gels and films applied in this study, including analysis of e.g., light absorbance (UV-vis spectroscopy of CNF gels), crystallinity (wide-angle X-ray scattering), zeta potential, viscosity, thermal properties (thermo-gravimetric analysis) of bleached samples from the same pulp, and pre-treated with the same amount of NaClO as bCNF_3.8 and bCNF_6.0 [17]. Additionally, the chemical structure (Fourier-transform infrared spectroscopy) and nano-characteristics (atomic force microscopy) of the same unbleached and bleached samples assessed in this study (uCNF_6.0 and bCNF_6.0) were provided [23].

In the present study, conductometric titration was applied to quantify the content of carboxylic acids of CNF gels (Table 1). The carboxyl acid content was 1023 ± 81 , 1061 ± 20 , 1356 ± 96 and 1435 ± 57 μ mol/g for the samples uCNF_3.8, bCNF_3.8, uCNF_6.0 and bCNF_6.0, respectively.

Self-standing films (20 g/ m^2) were made from the 4 CNF gels (Fig. 3), to complement previous assessments. CNF films are adequate for assessing various properties of the CNFs and provide a good indication of the nanofibrillation degree [36,37]. The more translucent the films, the higher the nanofibrillation [38]. The thermal and mechanical properties of the films are presented in Supplementary Table S1 and Table S2. No major differences were detected with respect to the decomposition

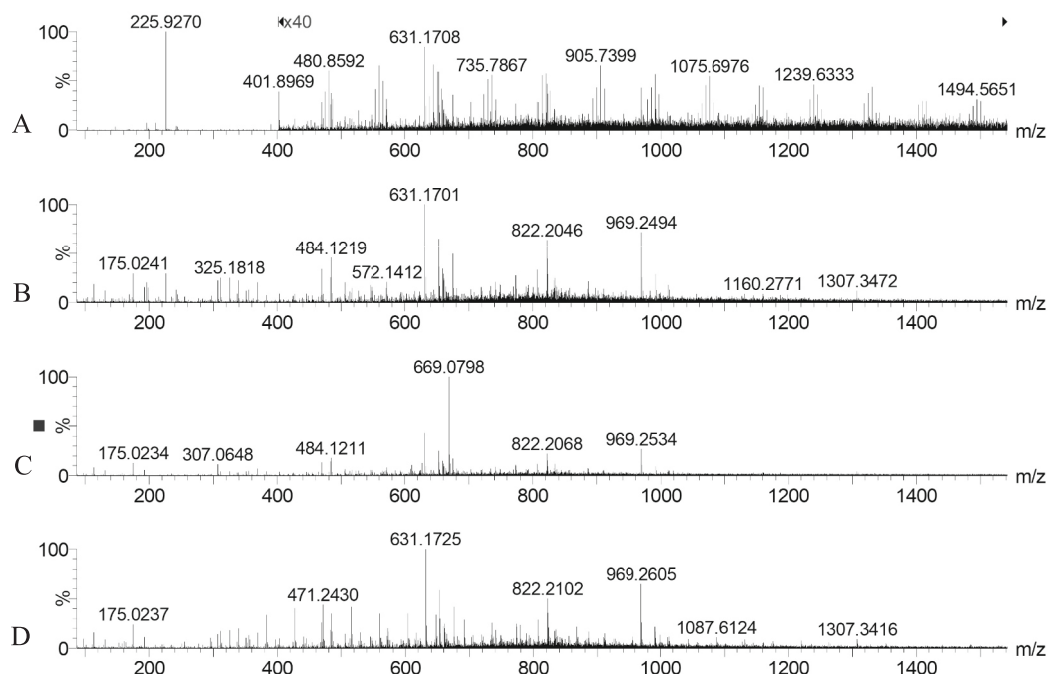


Fig. 4. ESI-MS in negative mode of (A) uCNF_3.8, (B) bCNF_3.8, (C) uCNF_6.0 and (D) bCNF_6.0.

temperature of the films (Supplementary Table S1). However, the films appeared to be brittle and with relatively low strength compared to previous studies [37]. The relatively low strength may be due to a potential degradation of the TEMPO CNFs with time [39]. On the other

hand, Tarrés et al. [40] also quantified the strength of TEMPO CNF films which varied between 90 and 153 MPa depending on the degree of nanofibrillation, and these strength values are in the range of the tensile strength quantified in this study (Supplementary Table S2). These

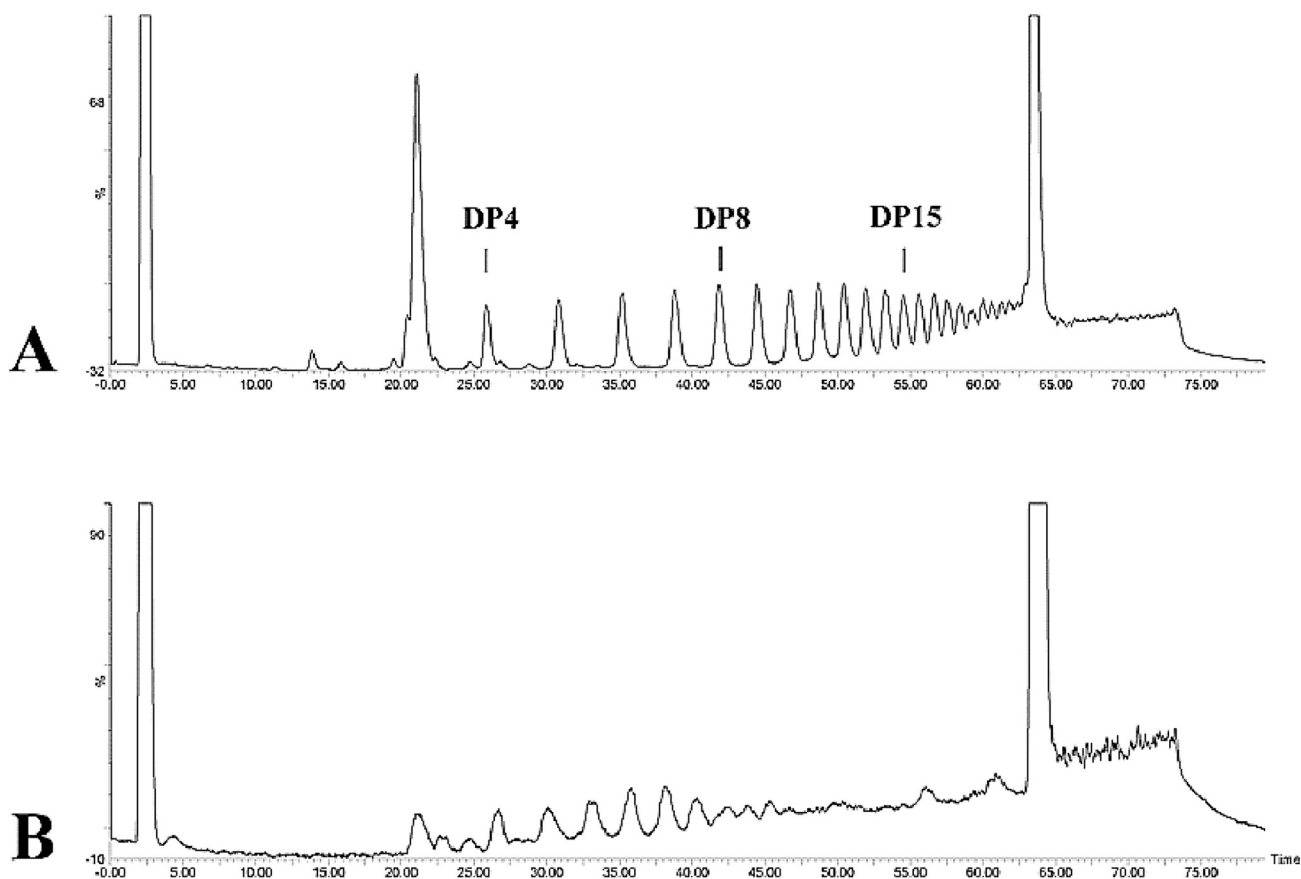


Fig. 5. (A) HPAEC Chromatogram of the mixture of oligouronates used as reference and (B) HPAEC chromatogram obtained by HCl hydrolysis of sample bCNF_6.0.

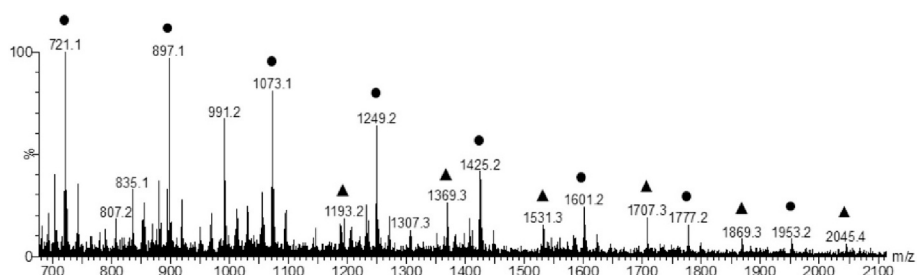


Fig. 6. MALDI-MS in negative mode of the mixture obtained by HCl hydrolysis of bCNF_6.0: ● correspond to homogluconic oligosaccharides and ▲ to alternating GlcA-Glc oligosaccharides.

analyses are important to provide more information on the effect of carboxyl acid content and degree of nanofibrillation on the potential occurrence of oligosaccharides. The hypothesis was that higher carboxyl acid content caused more nanofibrillated CNFs and larger occurrence of oligosaccharides.

Visual observation revealed that the uCNF_3.8 film (lowest strength) is more wrinkled, opaque and brownish than the other films (Fig. 3A). This is due to the less nanofibrillation of this sample and also due to the lignin content. As expected, the most translucent film is bCNF_6.0. This film has the highest carboxylation level (1435 $\mu\text{mol/g}$). The UV-vis transmittance analysis confirms the translucency of the samples with light transmittance levels of approx. 90 % (Fig. 3B), which is in accordance with the results of Fukuzumi et al. [37] who also demonstrated that the UV-vis transmittance of films corresponded well to the UV-vis transmittance of dispersions. Note that samples uCNF_3.8 and uCNF_6.0 contain lignin and this is the reason for light absorption in the UV-region (<400 nm wavelength). In addition, samples bCNF_3.8 and bCNF_6.0 reveal two distinct shoulders at 250 nm which is due to the aldehyde intermediates and carboxylation degree [36].

In order to provide more information of the CNF gels produced in this study, a detailed characterization was performed. High performance anionic exchange chromatography (HPAEC) is well-suited to analyze TEMPO oxidized CNF gels as it allows for the visualization of the different size (degree of polymerization, DP) of the oligosaccharides present in the CNF gel mixture. Further characterization can be obtained by mass spectrometry (MALDI-TOF and ESI) to reveal the corresponding

molecular mass. Moreover, MS/MS can provide additional information about these structures, in terms of sequence and composition [41–43]. The complementarity of these techniques will be explored in the following sections to provide a comprehensive description of the oligosaccharides.

Four samples of CNF gels were analyzed (Table 1). In order to detect possible oligosaccharides in the gels, these samples in gel form were directly analyzed by ESI-MS in the negative mode. The results are shown in Fig. 4. Some interesting oligosaccharide fragments are seen in all samples. The ESI-MS is operated in negative mode, and the fragments containing negatively charged gluconic acid (GlcA) residues are preferentially detected. A family of ions is clearly visible at m/z 822 (-2) \rightarrow 1307 (-1) \rightarrow 969 (-1) \rightarrow 631 (-1). The difference in mass units between the peaks is 338, which can be assigned to a glucose (Glc, 162 u) and a gluconic acid (176 u), revealing the presence of alternating [Glc-GlcA] $_n$ sequences. MS/MS analysis of m/z 822 (or its associated ions, Fig. S2) showed the successive losses of Glc and GlcA with DP of 9. From the peak at m/z 631, the loss of a Glc is also observed to give m/z 469. The loss of 132 u (corresponding probably to a pentose unit) led to m/z 337 and finally, a loss of another Glc gives the peak corresponding to GlcA (m/z 175). The presence of the pentose unit could be explained by the presence of the hemicellulose chains [44].

3.2. Characterization of the oligosaccharides obtained by acid hydrolysis

As bCNF_6.0 was the most nanofibrillated sample, it was selected for

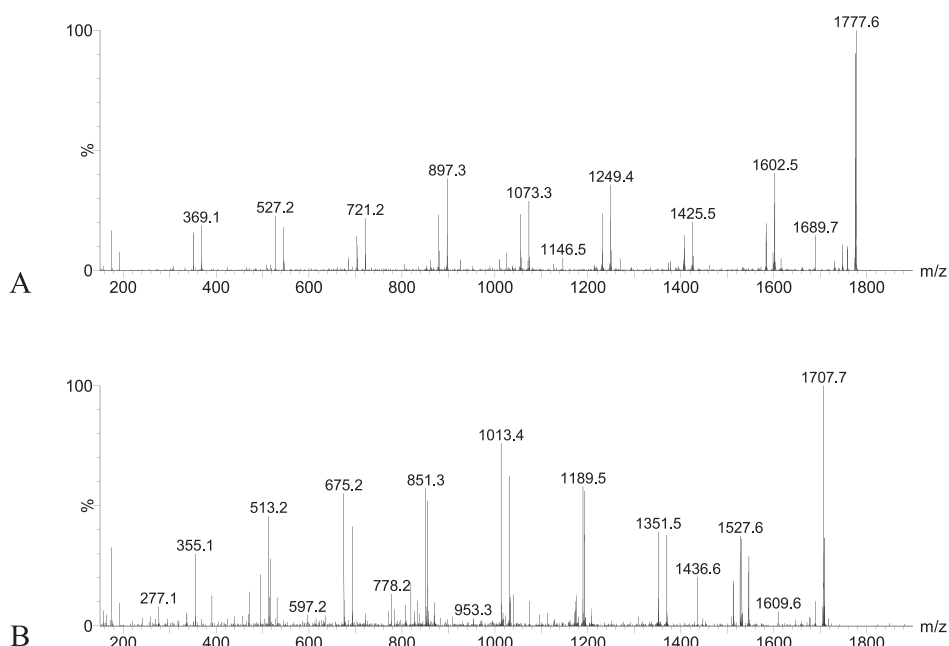


Fig. 7. MALDI-MS/MS in negative mode of m/z 1777 (A) and 1707 (B) ions.

further processing. Thus, acid hydrolysis of sample bCNF_6.0 was performed to obtain water-soluble oligosaccharides (20 % yield, Fig. 1). HPAEC in a DEAE column was performed to analyze the DP of the products obtained after acid-hydrolysis, in the pellet of sample bCNF_6.0 (water-soluble oligosaccharides, Fig. 1). Sample bCNF_6.0 was the most nanofibrillated (highest light transmittance, Fig. 3) and the oligosaccharides were more easily detected in this sample, confirming our hypothesis. The chromatogram of the water-soluble oligosaccharides is shown in Fig. 5. For comparison, a mixture of oligouronanes was chromatographed in the same conditions. The water-soluble oligosaccharides obtained from the bCNF_6.0 sample showed a mixture of oligosaccharides of different DP and charges. The presence of families other than regular oligouronanes was also evidenced.

In order to analyze the components of the oligosaccharides mixture, mass spectrometry in the negative mode was performed. Preliminary results revealed that MALDI-MS provided suitable characterization of the oligosaccharides mixture, where oligosaccharides with higher DP were clearly visible.

MALDI-TOF MS was performed using ionic liquid matrix of HABA/TMG₂ as matrix (Fig. 6). The signals corresponding to oligoglucuronic acids from DP4 to DP11 were observed at m/z 721, 897, 1073, 1249, 1425, 1601, 1777, 1953 as [M-H]. The second family of alternating Glc and GlcA residues (previously detected in the intact gel, Fig. 4) was also observed at m/z 1193, 1369, 1531, 1707, 1869 and 2045 corresponding to oligosaccharides (GlcA-Glc)_n from DP7 to DP12 respectively (Fig. S3 and S4). The presence of pentose units was not observed in these fragments, which can be explained by their lability during the hydrolysis.

Further characterization was performed by MALDI MS/MS of different peaks (Fig. 7). Fragmentation of peaks at m/z 1073 (DP6 GlcA) and 1777 (DP10 GlcA) showed the successive losses of 176 u corresponding to a GlcA. MS/MS of m/z 1707 assigned to (Glc-GlcA)₅ gave peaks at m/z 1527, 1351, 1189, 1013, 851, 675, 513, corresponding to the alternating losses of Glc and GlcA units (Fig. 7) as [M-H₂O-H]⁻¹. In addition, the peak at m/z 355 could be assigned to the disaccharide motive.

This result confirms that TEMPO oxidation would not occur randomly in the polysaccharide chain, but it would take place creating, on one hand, fully oxidized regions and on the other hand, regions where glucuronate units appear separated by untouched glucose residues. As Hirota et al. [45] previously reported, alternating glucose units in the polymer expose the OH-6 to the oxidant, *i.e.*, TEMPO would approach from one side of the linear-like chain, the other face being hindered. The authors observed these alternating Glc-GlcA oligosaccharides by NMR spectroscopy of the water-soluble oligosaccharides obtained by surface peeling with NaOH of TEMPO oxidized nanocellulose. Here, well-defined oligosaccharides were obtained by acid hydrolysis of TEMPO CNFs and confirmed for the first time the presence of these sequences by mass spectrometry.

Some minor peaks can be observed in the MALDI spectrum at m/z 1705 and 1029. Such peaks could be assigned to the presence of a 6-aldehyde replacing a Glc in these oligosaccharides, as expected from the intermediate aldehyde produced during the TEMPO oxidation reaction to carboxylic acid (Supporting information, Fig. S5). Still a peak at m/z 1055 suggests the presence of a lactone in a homogluconic acid hexasaccharide (Supporting information, Fig. S6).

Previously it has been reported that oligosaccharides with DP between 10 and 16 are produced by plants as response to biotic and abiotic stresses [3]. The oligosaccharides obtained in this study may constitute a new family of elicitors (with carboxylic acid and aldehyde groups) with potential of mass production. In order to explore the potential of CNF oligosaccharides as bioactive components (elicitors), the CNF gels were tested as substrate for growth of *C. annuum* plants, and the gene expression was evaluated after 2 weeks of growth.

Table 2

Approximate carbohydrate composition and lignin content of uCNF_3.8 and bCNF_3.8. The values of carbohydrates have been adjusted so the total sum of the components is 100 wt%.

| | uCNF_3.8 (wt%) | bCNF_3.8 (wt%) |
|-----------|----------------|----------------|
| Glucans | 85.2 ± 0.7 | 88.4 ± 0.1 |
| Xylans | 7.3 ± 0.2 | 6.0 ± 0.0 |
| Mannans | 3.8 ± 0.2 | 3.0 ± 0.2 |
| Rhamnans | 1.0 ± 0.0 | 0.9 ± 0.0 |
| Arabinans | 1.1 ± 0.2 | 1.2 ± 0.0 |
| Lignin | 1.7 ± 0.1 | 0.5 ± 0.2 |

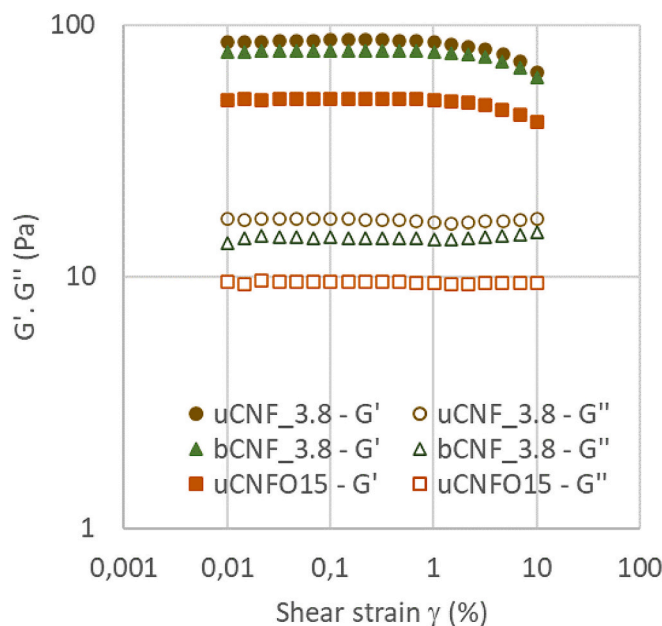


Fig. 8. Rheology analysis of samples uCNF_3.8, bCNF_3.8 and uCNFO15.

3.3. Gels as substrate for plant trials

Based on preliminary trials, samples uCNF_3.8 and bCNF_3.8 were selected for further testing as these samples showed a distinct growth pattern and required less chemicals to be produced. Sample bCNF_6.0 was more nanofibrillated and was thus applied for further production of oligosaccharides. To complement the study, the carbohydrate composition of the uCNF_3.8 and bCNF_3.8 samples is provided in Table 2. Note that the samples contain 85 and 88 wt% of glucans in addition to xylans, mannans, rhamnans and arabinans. Previously, it has been reported that using 3.8–5.0 mmol/g NaClO, during TEMPO-mediated oxidation, some co-oxidized hemicelluloses remained, which agrees with our study [46]. Oxidized TEMPO penetrates easily into the hemicellulose-rich areas and this seems to facilitate the nanofibrillation of cellulose fibers [15]. The unbleached CNFs (uCNF_3.8 and uCNF_6.0) also contain lignin (Fig. 3), but less than in the raw kraft pulp (Table 2) as hemicellulose and lignin are removed due to the consumption of NaClO during TEMPO-mediated oxidation [15]. Additionally, due to the bleaching process which removes most of the lignin, the relative fraction of glucans increases and this also reduces the fraction of xylans from 7.3 to 6.0 wt% for the uCNF_3.8 and bCNF_3.8, respectively.

The rheology of the gels uCNF_3.8 and bCNF_3.8 is given in Fig. 8. At shear strain below 1 % the storage (G') and loss (G'') moduli are relatively constant and the CNFs reveal gel-like properties ($G' > G''$). Similar results have previously been obtained for TEMPO CNFs at concentrations of 0.56 wt% [47] and 1.0 wt% [48]. The G' and G'' of sample uCNFO15 (85 wt% uCNF_3.8 with 15 wt% of the water-soluble oligosaccharides from sample bCNF_6.0, Fig. 1) are lower compared to the

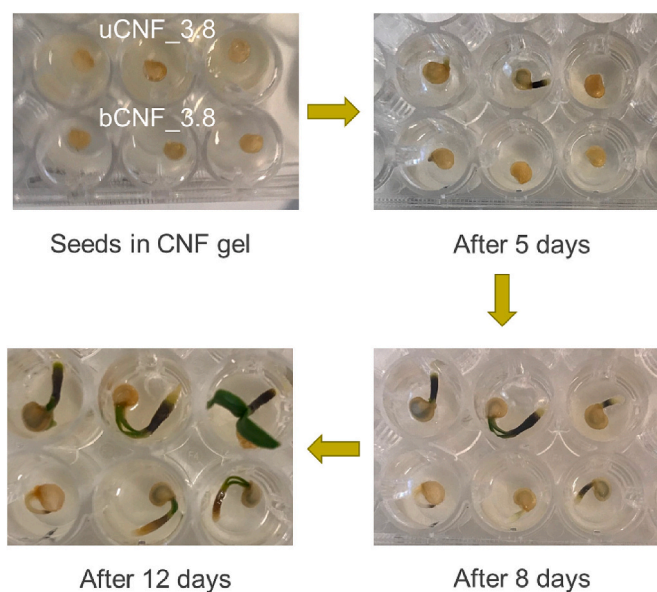


Fig. 9. Cultivation of *C. annuum* seeds in CNF gels over 12 days.

other two CNF gels (uCNF_3.8 and bCNF_3.8), due to the higher amount of low molecular weight oligosaccharides which causes lower viscosity and weaker gel.

3.4. Analysis of gene expression

C. annuum seeds were grown in soil (control) and three different CNF gels, i.e. uCNF_3.8, bCNF_3.8 and uCNF_3.8 complemented with 15 % oligosaccharides (uCNFO15). The growth of the plants after two weeks was visually assessed (Fig. 9). The growth of the soil-grown plants exceeded that of the CNF-grown plants. However, there were differences in the growth patterns between the CNF-gels as well, i.e., the seeds grew better in uCNF_3.8 as compared to the other gels. This may be attributed to the chemical composition of the gels. The uCNF_3.8 sample contained more lignin and a larger fraction of hemicelluloses, compared to the bCNF_3.8 (Table 2). Previously, it has been reported that xylan increased the G' and G'' of TEMPO oxidated CNFs [49], which is in agreement with our study, when comparing uCNF_3.8 with bCNF_3.8 (Fig. 8). It's important to emphasize that the CNF gels had a concentration of 0.6 wt %, i.e., 99.4 wt% water. There was no growth when the seeds were placed in 100 % water. Hence, CNF gels with only 0.6 % dry matter (including nanofibrils and oligosaccharides) contributed to providing a good microenvironment for the seeds to germinate and grow. The steps for RNA extraction, sequencing and analysis are schematically described in Fig. 2.

Gene expression analysis with RNA-sequencing showed upregulation of 29 genes in all three CNF-grown samples in comparison to the control, while 46 genes were downregulated (Fig. 10). In the uCNF_3.8 sample the majority of the differentially expressed genes were downregulated; 934 vs 78 genes. However, in contrast to the uCNF_3.8 samples, in both the bCNF_3.8 and uCNFO15 samples the differentially expressed genes were almost equally distributed between up and down-regulation. In addition, the expression pattern of the bCNF_3.8 and uCNFO15 samples

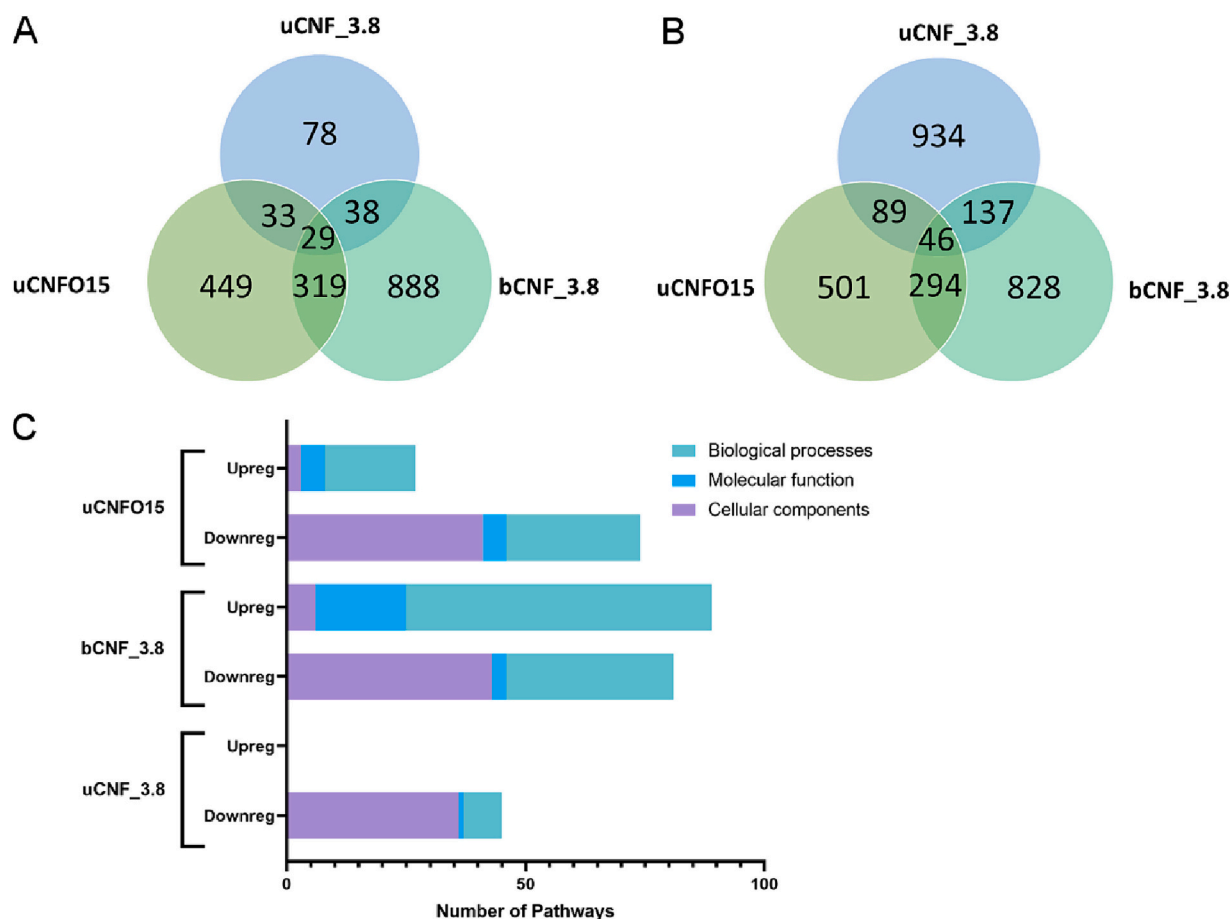


Fig. 10. Number of (A) upregulated genes, (B) downregulated genes in comparison with control samples and (C) number of upregulated and down-regulated pathways.

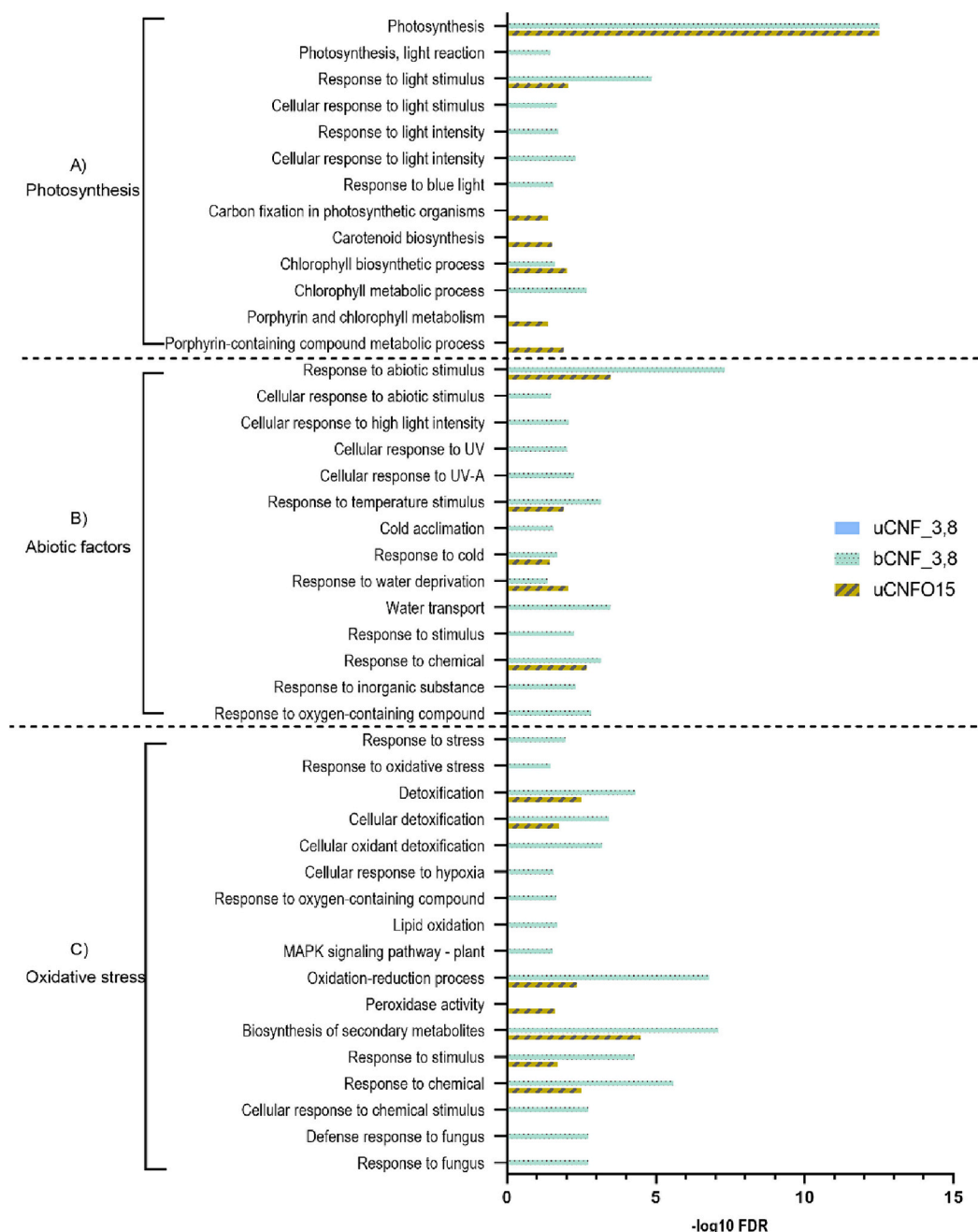


Fig. 11. Pathway analysis of (A) photosynthesis, (B) abiotic factors and (C) oxidative stress.

partially overlapped, even though the actual number of differentially expressed genes were higher in the bCNF_3.8 samples. It is noteworthy to mention that uCNFO15 was composed of uCNF_3.8 (85 wt%) and only 15 wt% oligosaccharides from bCNF_6.0. Additionally, despite major differences between the rheological properties between the samples (G'' of uCNFO15 $<<$ G'' bCNF_3.8, Fig. 8), the bCNF_3.8 and uCNFO15 samples partially overlapped (Fig. 10). We thus expect that the gel strength was not a major cause of the obtained results regarding gene expression.

3.5. Pathway analysis

As expected from the differentially expressed genes (Fig. 10), the pathways analysis showed large differences between the different CNF-grown samples. While the main effects for uCNF_3.8 grown samples were on downregulation on pathways regulating cellular components

and to some extent metabolic processes (Fig. 10C), the other two CNF-grown samples were also affected when it comes to biological processes. Since the bCNF_3.8-grown samples had the largest number of differentially expressed genes the effects on regulatory pathways were also the most extensive for these samples.

When it comes to regulation of photosynthesis (Fig. 11A), both the bCNF_3.8 and the uCNFO15-grown samples showed a downregulation of regulating pathways. For the bCNF_3.8-grown samples the downregulation was more prominent than for the uCNFO15-grown samples. The modulus G'' (which is related to the viscosity of the gels) does not seem to affect the regulation of photosynthesis as the G'' levels follow the sequence uCNF_3.8 $>$ bCNF_3.8 $>>$ uCNFO15 (Fig. 8) and may be an indication that the chemical composition of the gels (carbohydrates and lignin) is the predominant effect on the growth pattern of the plants. The visually assessed growth pattern of the plants grown in uCNF_3.8 over 12 days (Fig. 9) also correlated well with the extent of downregulation of

the photosynthetic pathways. Thus, this seems to confirm the positive effect of the uCNF 3.8 sample on plant growth as uCNFO15 contains 85 wt% uCNF 3.8 and this gel caused the quickest growth during the first two weeks of cultivation (Fig. 9).

Regulation of response to abiotic factors (Fig. 11B) were also downregulated in both bCNF 3.8 and uCNFO15-grown samples. In both types of samples, responses to temperature, in particular to cold, water deprivation and chemicals were affected. For bCNF 3.8 there was also an effect of regulation of the response to UV-light and light intensity in general.

Pathways regulating oxidative stress and detoxification (Fig. 11C) were on the other hand upregulated in both the bCNF 3.8 and uCNFO15-grown samples. The upregulation of oxidative stress signal might be due to some effects of the bleaching process as no such upregulation is seen in the samples grown in the unbleached gel (uCNF 3.8). We hypothesize that this is due to the lignin content as lignin is a known antioxidant and the uCNF 3.8 gel contained more lignin (Table 2). As for the photosynthesis pathways, the differential expression was most pronounced for the bCNF 3.8-grown samples.

Finally, the potential of RNA sequencing of the *C. annuum* plant's total mRNA using NGS has been demonstrated. The technology contributed to assess the potential effect TEMPO CNF gels and, specifically, oligosaccharides have on various physiological processes (e.g. photosynthesis, oxidative stress) and abiotic factors. Moreover, reverse transcription-quantitative polymerase chain reaction (RT-qPCR) could be used to validate the results presented in this study. However, RT-qPCR validation would require functional studies and where RT-PCR on selected genes can be combined with protein expression studies. Additional functional studies may also benefit from the shear thinning behavior of TEMPO CNF gels at low concentration [50] may also facilitate the application of CNFs by spraying. This is considered a more feasible application method in large plant trials. Therefore, although the methodology described in this study (CNFs as substrate) is expected to provide a more rapid screening of elicitor candidates, sprayable CNF gels may be more appropriate for large plant trials and functional studies.

4. Conclusion

The composition of TEMPO oxidized CNF gels with and without lignin was analyzed at the molecular level, first in the gel form, and then after acid hydrolysis to give a mixture of oligosaccharides. In addition to the expected homogalacturonic acid series a second family of alternating Glc and GlcA residues was clearly identified by mass spectrometry. The TEMPO CNF gels were combined with oligosaccharides (from bleached TEMPO CNF) to test the elicitor potential on Chili plants (*C. annuum*).

The differences in growth of the CNF-gel grown *C. annuum* seeds correlate well with the downregulation of the pathways regulating photosynthesis, where CNF containing lignin caused the most favorable conditions for growth during the testing period, compared to bleached CNF without lignin.

The observed downregulation of the response to abiotic factors, in the plants grown in bCNF 3.8-gels, could result in the plants being less sensitive to such stimuli. Consequently, making the plants more resistant to, e.g., water deprivation and cold temperatures, compared to plants grown in conventional soil.

It remains to be determined whether the downregulation of the response to abiotic stimuli is due to the upregulation of the oxidative stress response or a true effect of the cellulose substrate. Concluding, to further investigate the impact of the CNF-gels on the response to abiotic factors, functional studies need to be conducted.

CRedit authorship contribution statement

María Emilia Cano: Writing – review & editing, Writing – original draft, Visualization, Validation, Methodology, Investigation, Data

curation. **Åsa Lindgren:** Writing – review & editing, Visualization, Validation, Methodology, Investigation, Data curation. **Jennifer Rosen-dahl:** Writing – review & editing, Visualization, Validation, Methodology, Investigation, Data curation. **Jenny Johansson:** Validation, Methodology, Data curation. **Alberto Garcia-Martin:** Writing – review & editing, Methodology, Data curation. **Miguel Ladero Galan:** Writing – review & editing, Supervision, Project administration, Methodology, Funding acquisition, Data curation. **José Kovensky:** Writing – review & editing, Validation, Supervision, Methodology, Investigation, Data curation. **Gary Chinga-Carrasco:** Writing – review & editing, Writing – original draft, Visualization, Validation, Supervision, Resources, Project administration, Methodology, Investigation, Funding acquisition, Data curation, Conceptualization.

Declaration of competing interest

The authors declare that they have no known competing financial interests or personal relationships that could have appeared to influence the work reported in this paper.

Data availability

Data will be made available on request.

Acknowledgment

The Research Council of Norway (Grant no. 284300), ANR (France, Grant ANR-18-SUS2-0001), MINECO (Spain, Grant PCI2018-093114) and SUSFOOD2 ERA-NET program (Grant SPAREC) are acknowledged for funding. Mirjana Filipovic, Ingebjørg Leirset, Johnny Kvakland Melbø, Kenneth Aasarød (RISE PFI) and Simon Standoft (RISE) are acknowledged for excellent laboratory work.

Appendix A. Supplementary data

Supplementary data to this article can be found online at <https://doi.org/10.1016/j.ijbiomac.2024.131229>.

References

- [1] J. Eder, E.G. Cosio, Elicitors of plant defense responses, in: K.W. Jeon, J. Jarvik (Eds.), *International Review of Cytology*, Academic Press, 1994, pp. 1–36.
- [2] S. Ferrari, D. Savatin, F. Sicilia, G. Gramegna, F. Cervone, G. De Lorenzo, Oligogalacturonides: plant damage-associated molecular patterns and regulators of growth and development, *Front. Plant Sci.* 4 (2013).
- [3] I.A. Larskaya, T.A. Gorshkova, Plant oligosaccharides - outsiders among elicitors? *Biochemistry (Mosc.)* 80 (7) (2015) 881–900.
- [4] F. Zheng, L. Chen, P. Zhang, J. Zhou, X. Lu, W. Tian, Carbohydrate polymers exhibit great potential as effective elicitors in organic agriculture: a review, *Carbohydr. Polym.* 230 (2020) 115637.
- [5] E.F. Abouraicha, Z. El Alaoui-Talibi, A. Tadiaoui-Ouafi, R. El Boutachfaiti, E. Petit, A. Douira, B. Courtois, J. Courtois, C. El Modafar, Glucuronan and oligogalacturonans isolated from green algae activate natural defense responses in apple fruit and reduce postharvest blue and gray mold decay, *J. Appl. Phycol.* 29 (1) (2017) 471–480.
- [6] S. Caillot, S. Rat, M.-L. Tavernier, P. Michaud, J. Kovensky, A. Wadouachi, C. Clément, F. Baillieul, E. Petit, Native and sulfated oligogalacturonans as elicitors of defence-related responses inducing protection against *Botrytis cinerea* of *Vitis vinifera*, *Carbohydr. Polym.* 87 (2) (2012) 1728–1736.
- [7] S. Pring, H. Kato, S. Imano, M. Camagna, A. Tanaka, H. Kimoto, P. Chen, A. Shrotri, H. Kobayashi, A. Fukuoka, M. Saito, T. Suzuki, R. Terauchi, I. Sato, S. Chiba, D. Takemoto, Induction of plant disease resistance by mixed oligosaccharide elicitors prepared from plant cell wall and crustacean shells, *Physiol. Plant.* 175 (5) (2023) e14052.
- [8] M.E. Cano, A. García-Martin, P. Comendador Morales, M. Wojtusik, V.E. Santos, J. Kovensky, M. Ladero, Production of oligosaccharides from Agrofood wastes, *Fermentation* 6 (1) (2020) 31.
- [9] N. Sato, Y. Takano, M. Mizuno, K. Nozaki, S. Umemura, T. Matsuzawa, Y. Amano, S. Makishima, Production of feruloylated arabino-oligosaccharides (FA-AOs) from beet fiber by hydrothermal treatment, *J. Supercrit. Fluids* 79 (2013) 84–91.
- [10] M.E. Cano, A. García-Martin, M. Ladero, D. Lesur, S. Pilard, J. Kovensky, A simple procedure to obtain a medium-size oligogalacturonic acids fraction from orange peel and apple pomace wastes, *Food Chem.* 346 (2021) 128909.

- [11] L. Lehuedé, C. Henríquez, C. Carú, A. Córdova, R.T. Mendonça, O. Salazar, Xylan extraction from hardwoods by alkaline pretreatment for xylooligosaccharide production: a detailed fractionation analysis, *Carbohydr. Polym.* 302 (2023) 120381.
- [12] F.A. de Moura, F.T. Macagnan, L.P. da Silva, Oligosaccharide production by hydrolysis of polysaccharides: a review, *Int. J. Food Sci. Technol.* 50 (2) (2015) 275–281.
- [13] T. Saito, A. Isogai, TEMPO-mediated oxidation of native cellulose. The effect of oxidation conditions on chemical and crystal structures of the water-insoluble fractions, *Biomacromolecules* 5 (5) (2004) 1983–1989.
- [14] T. Saito, A. Isogai, Introduction of aldehyde groups on surfaces of native cellulose fibers by TEMPO-mediated oxidation, *Colloids Surf. A Physicochem. Eng. Asp.* 289 (1) (2006) 219–225.
- [15] A. Isogai, T. Saito, H. Fukuzumi, TEMPO-oxidized cellulose nanofibers, *Nanoscale* 3 (1) (2011) 71–85.
- [16] R. Shinoda, T. Saito, Y. Okita, A. Isogai, Relationship between length and degree of polymerization of TEMPO-oxidized cellulose Nanofibrils, *Biomacromolecules* 13 (3) (2012) 842–849.
- [17] G. Chinga-Carrasco, J. Johansson, E.B. Heggset, I. Leirset, C. Björn, K. Agrenius, J. S. Stevanic, J. Håkansson, Characterization and antibacterial properties of autoclaved Carboxylated wood Nanocellulose, *Biomacromolecules* 22 (7) (2021) 2779–2789.
- [18] H.R. Nordli, G. Chinga-Carrasco, A.M. Rokstad, B. Pukstad, Producing ultrapure wood cellulose nanofibrils and evaluating the cytotoxicity using human skin cells, *Carbohydr. Polym.* 150 (2016) 65–73.
- [19] A.L. Basu, E. Ålander, M. Strømme, N. Ferraz, On the use of ion-crosslinked nanocellulose hydrogels for wound healing solutions: physicochemical properties and application-oriented biocompatibility studies, *Carbohydr. Polym.* 174 (2017) 299–308.
- [20] X. Lan, Z. Ma, A.R.A. Szojka, M. Kunze, A. Mulet-Sierra, M.J. Vyhldal, Y. Boluk, A. B. Adesida, TEMPO-oxidized cellulose nanofiber-alginate hydrogel as a bioink for human Meniscus tissue engineering, *Front. Bioeng. Biotechnol.* 9 (2021).
- [21] A. Rashad, S. Suliman, M. Mustafa, T.Ø. Pedersen, E. Campodoni, M. Sandri, K. Syverud, K. Mustafa, Inflammatory responses and tissue reactions to wood-based nanocellulose scaffolds, *Mater. Sci. Eng. C* 97 (2019) 208–221.
- [22] H. Zhang, M. Yang, Q. Luan, H. Tang, F. Huang, X. Xiang, C. Yang, Y. Bao, Cellulose anionic hydrogels based on cellulose nanofibers as natural stimulants for seed germination and seedling growth, *J. Agric. Food Chem.* 65 (19) (2017) 3785–3791.
- [23] B.H. McDonagh, G. Chinga-Carrasco, Characterization of porous structures of cellulose nanofibrils loaded with salicylic acid, *Polymers* 12 (11) (2020) 2538.
- [24] Y. Bektas, T. Eulgem, Synthetic plant defense elicitors, *Front. Plant Sci.* 5 (2015).
- [25] H.A. Chowdhury, D.K. Bhattacharyya, J.K. Kalita, Differential expression analysis of RNA-seq reads: overview, taxonomy, and tools, *IEEE/ACM Trans Comput Biol Bioinform* 17 (2) (2020) 566–586.
- [26] T.L. Olatunji, A.J. Afolayan, The suitability of chili pepper (*Capsicum annum* L.) for alleviating human micronutrient dietary deficiencies: a review, *Food Sci. Nutr.* 6 (8) (2018) 2239–2251.
- [27] D. Ozdemir, Here's how NASA astronauts grew perfect peppers on the ISS, in: *Interesting Engineering*, 2022.
- [28] T. Hosoya, M. Bacher, A. Potthast, T. Elder, T. Rosenau, Insights into degradation pathways of oxidized anhydroglucose units in cellulose by β -alkoxy-elimination: a combined theoretical and experimental approach, *Cellulose* 25 (7) (2018) 3797–3814.
- [29] J. Milanovic, S. Schiehser, P. Milanovic, A. Potthast, M. Kostic, Molecular weight distribution and functional group profiles of TEMPO-oxidized lyocell fibers, *Carbohydr. Polym.* 98 (1) (2013) 444–450.
- [30] T.I. Saito, TEMPO-mediated oxidation of native cellulose. The effect of oxidation conditions on chemical and crystal structures of the water-insoluble fractions, *Biomacromolecules* 5 (5) (2004) 1983–1989.
- [31] A.H. Sluiter, Ruiz, R.; Scarlata, C.; Sluiter, J.; Templeton, D.; Crocker D., Determination of structural carbohydrates and lignin in biomass, NREL Laboratory analytical procedure, National Renewable Energy Laboratory, 2008, p. 18.
- [32] B.R. Hames, C. Scarlata, A. Sluiter, J. Sluiter, D. Templeton, Preparation of samples for compositional analysis, in: NREL Laboratory Analytical Procedure, 2008, p. 12.
- [33] S. Aziz, TAPPI T 236: Kappa Number of Pulp., TAPPI—Test Methods, 2006, p. 23.
- [34] D.W. Armstrong, L.-K. Zhang, L. He, M.L. Gross, Ionic liquids as matrices for matrix-assisted laser desorption/ionization mass spectrometry, *Anal. Chem.* 73 (15) (2001) 3679–3686.
- [35] C. Przybylski, F. Gonnert, D. Bonnaffé, Y. Hersant, H. Lortat-Jacob, R. Daniel, HABA-based ionic liquid matrices for UV-MALDI-MS analysis of heparin and heparan sulfate oligosaccharides, *Glycobiology* 20 (2) (2010) 224–234.
- [36] H. Fukuzumi, T. Saito, T. Iwata, Y. Kumamoto, A. Isogai, Transparent and high gas barrier films of cellulose nanofibers prepared by TEMPO-mediated oxidation, *Biomacromolecules* 10 (1) (2009) 162–165.
- [37] H. Fukuzumi, T. Saito, A. Isogai, Influence of TEMPO-oxidized cellulose nanofibril length on film properties, *Carbohydr. Polym.* 93 (1) (2013) 172–177.
- [38] G. Chinga-Carrasco, Optical methods for the quantification of the fibrillation degree of bleached MFC materials, *Micron* 48 (2013) 42–48.
- [39] J. Milanovic, S. Schiehser, A. Potthast, M. Kostic, Stability of TEMPO-oxidized cotton fibers during natural aging, *Carbohydr. Polym.* 230 (2020) 115587.
- [40] Q. Tarrés, S. Boufi, P. Mutjé, M. Delgado-Aguilar, Enzymatically hydrolyzed and TEMPO-oxidized cellulose nanofibers for the production of nanopapers: morphological, optical, thermal and mechanical properties, *Cellulose* 24 (9) (2017) 3943–3954.
- [41] Y. Mechref, M.V. Novotny, C. Krishnan, Structural characterization of oligosaccharides using MALDI-TOF/TOF tandem mass spectrometry, *Anal. Chem.* 75 (18) (2003) 4895–4903.
- [42] Q. Yang, Y. Guo, Y. Jiang, B. Yang, Structure identification of the oligosaccharides by UPLC-MS/MS, *Food Hydrocoll.* 139 (2023) 108558.
- [43] A. Voxeur, O. Habrylo, S. Guénin, F. Miar, M.-C. Soulié, C. Rihouey, C. Pau-Roblot, J.-M. Doman, L. Gutierrez, J. Pelloux, G. Mouille, M. Fagard, H. Höfte, S. Vernhettes, Oligogalacturonide production upon *Arabidopsis thaliana*-*Botrytis cinerea* interaction, *Proc. Natl. Acad. Sci.* 116 (39, 2019) 19743–19752.
- [44] O. Obembe, E. Jacobsen, R.G.F. Visser, J.P. Vincken, Cellulose-hemicellulose networks as target for in planta modification of the properties of natural fibres, *Biotechnology and Molecular Biology Review* 1 (3) (2006) 76–86.
- [45] M. Hirota, K. Furihata, T. Saito, T. Kawada, A. Isogai, Glucose/glucuronic acid alternating co-polysaccharides prepared from TEMPO-oxidized native celluloses by surface peeling, *Angew. Chem. Int. Ed.* 49 (42) (2010) 7670–7672.
- [46] R. Hiraoki, Y. Ono, T. Saito, A. Isogai, Molecular mass and molecular-mass distribution of TEMPO-oxidized celluloses and TEMPO-oxidized cellulose Nanofibrils, *Biomacromolecules* 16 (2) (2015) 675–681.
- [47] R. Aaen, S. Simon, F. Wernersson Brodin, K. Syverud, The potential of TEMPO-oxidized cellulose nanofibrils as rheology modifiers in food systems, *Cellulose* 26 (9) (2019) 5483–5496.
- [48] O. Nechyporchuk, M.N. Belgacem, F. Pignon, Concentration effect of TEMPO-oxidized nanofibrillated cellulose aqueous suspensions on the flow instabilities and small-angle X-ray scattering structural characterization, *Cellulose* 22 (4) (2015) 2197–2210.
- [49] T. Pääkkönen, K. Dimic-Misic, H. Orelma, R. Pönni, T. Vuorinen, T. Maloney, Effect of xylan in hardwood pulp on the reaction rate of TEMPO-mediated oxidation and the rheology of the final nanofibrillated cellulose gel, *Cellulose* 23 (1) (2016) 277–293.
- [50] Y. Liu, K. Gordeyeva, L. Bergström, Steady-shear and viscoelastic properties of cellulose nanofibril–nanoclay dispersions, *Cellulose* 24 (4) (2017) 1815–1824.